

A DESCRIPTION OF THE VELOCITY FIELD OF A VANE EXCITED JET

W.H. HARCH WITH D.J. COLLINS & M.F. PLATZER

AERONAUTICAL RESEARCH LABS
FISHERMAN'S BEND
VIC. 3207 AUSTRALIA

U.S. NAVAL POSTGRAD. SCHOOL
MONTEREY, CA. 93940 U.S.A.

ABSTRACT A series of Laser Doppler Anemometer measurements was made to characterize the velocity field of a two dimensional subsonic air jet exhausting to atmosphere. The jet was excited by a small vane oscillating in pitch and located in the potential core region of the jet. Profiles of mean velocities, Reynolds stress components and entrainment are presented.

1 INTRODUCTION

The mixing and entrainment characteristics of turbulent jets have long been a subject of basic and applied interest in fluid mechanics. Recently, the enhancement of jet flow entrainment has attracted increased attention because of the need to develop compact, yet efficient, thrust augmenting ejectors for aerospace propulsion systems, particularly for V/STOL aircraft applications. The energy exchange from a primary flow, such as a jet, to the surrounding fluid, can be accomplished by either viscous interactions (characterized by considerable mixing of the two fluids) or by pressure forces across the interface (characterized by little mixing). To increase the efficiency of the energy transfer process experimenters have utilized methods ranging from a simple corrugated nozzle to increase the size of the mixing shear layer to pulsed primary flow, which relies principally on energy transfer by pressure forces. In between these extremes, experimenters have attempted to excite the flow by mechanical, acoustic, and fluidic means. The problem facing all these methods has been the trade-off between increased entrainment (and consequently high augmentation ratio) and increased primary nozzle losses that accompany many jet excitation schemes.

The following jet excitation scheme was adopted in the hope of achieving a good compromise between enhanced jet entrainment and decreased nozzle efficiency. The scheme utilized a small vane which was situated in the jet potential core and which was excited into small pitch oscillations such that both frequency and amplitude of oscillation could be varied over a significant range. The investigation of this type of jet excitation was stimulated by the encouraging results reported by Fiedler and Korschelt (1979) who used a freely vibrating vane for jet excitation. The experiments reported in the following sections follow on from the earlier work of Collins, et al (1981).

2 TEST CONFIGURATION

Velocity measurements were made in a vane excited jet of air which issued into stationary air from a plenum chamber through a rectangular nozzle of length $L = 300\text{mm}$ and width $d = 6\text{mm}$. Wire gauzes and honeycombs were installed upstream of the nozzle to reduce the turbulence at the jet exit. No side plates were used to contain the jet. The chamber pressure and temperature were continuously monitored during the experiments through a manometer and a thermocouple respectively.

A vane which had a symmetrical airfoil section with a thickness of 1.3mm, a span of 360mm and chord of 10mm was located symmetrically in the potential core at 1.42d from the nozzle. The vane was oscillated in pitch with variable frequency and amplitude about a mean position set at zero angle of attack. To reduce the vane's

tendency to flutter at high nozzle pressure ratios, it was supported with two bearings 123mm apart, reducing the nozzle's aspect ratio to an effective value of 1:20. This aspect ratio is still considered acceptable for two-dimensional jets, e.g. Goldschmidt and Eskinazi (1965).

The velocity measurements were made across the width of the jet at its midspan and at distances x of 20, 30, 40, 50 and 60 nozzle widths downstream for the following conditions.

- Nozzle Pressure Ratio P_r (Plenum Chamber Pressure/ Atmospheric Pressure) = 1.137
- Jet Exit Reynolds Number base on jet width 5.85×10^4
- Vane Amplitude of Oscillation (zero-peak) 6.9°
- Vane Frequency of Oscillation (f) OHZ, 40Hz

Additional measurements were made at $x/d = 40$ for vane frequencies of 20Hz, 30Hz and pressure ratios of 1.008 and 1.268.

3 LASER DOPPLER VELOCIMETER (LDV)

The LDV was a DISA two component, two color, three beam differential doppler system operating in the forward scatter mode with photomultiplier tubes in an approximately axial position for detection of particle signals. Orthogonal Velocity Components were measured $\pm 45^\circ$ to the jet axes in the plane normal to the jet exit plane. Seeding particles, generated by a TSI Model 3075 constant output atomizer, were seeded at a rate of 0.3 cc/min in the plenum chamber upstream of the nozzle. Particle sizes, though variable, never exceeded $1\mu\text{m}$. Dynamic calibrations indicate that the seed particles will track the flow with a relaxation time of the order 10^{-6} sec. The fringe spacing was of the order 17 times greater than particle size; this is within the range indicated by Durst, et al (1976) to produce acceptable bandpass filtered doppler signals.

The counters were operated in the 5:8 comparison mode (6% error limit). Digital counter data were fed into a DISA 57G20 Buffer Interface. The Buffer contained a 1K buffer register and coincidence filter and dual-timing boards for preprocessing the signal. The coincidence filter board blocked the input multiplexer if data were not presented at both channels within a predetermined coincidence time window. For these experiments this window was the time required for a 5:8 doppler frequency count for the lowest velocity of interest. The dual timing board enabled the measurement of the time that each velocity reading occurred with respect to a triggering event, which was a pulse produced when the vane was in the horizontal position with decreasing angle of attack.

Buffer output signals were further reduced by an on-line HP 9825B microcomputer. The computer software enabled digital filtering of received doppler signals, the selected plotting of histograms of measured doppler frequency distributions, the resolution of the measured coincident velocities into axial (U) and cross flow (V) components, and the evaluation and storage of average quantities \bar{U} , \bar{U}^2 , \bar{U}^3 , \bar{U}^4 , \bar{V} , \bar{V}^2 , \bar{V}^3 and \bar{UV} sampled either on a continuous or a conditional basis.

4 EXPERIMENTAL RESULTS

4.1 Effect of Vane

A stationary vane placed at zero angle of attack in the jet potential core has little effect on the flow at distances remote from the vane itself. This was determined from measurements taken of the mean velocity components and the Reynolds stress tensor at $x/d = 20$ for the vane present and vane absent situations.

4.2 Comparison of Stationary Vane with Other Plane Jets

Measurements were taken at all locations with the vane stationary to check for self preservation and consistency with other reported data for turbulent plane jets. Plots of mean axial velocity, \bar{U} , normalized on centreline value U_m , against normalized distance from jet centreline, y/b (Fig. 1) show that self preservation occurs for $x/d > 20$. The profiles agree with the Goertler solution for a plane jet, equation 1, with the usual discrepancy at the edge of the jet

$$\frac{\bar{U}}{U_m} = 1 - \tanh^2 \frac{\sigma y}{x} \quad (1)$$

The centreline mean velocity decay and the growth of the jet half width b (Value of y at which $\bar{U} = 0.5 U_m$) can be modelled by equations 2 and 3 respectively.

$$\frac{b}{d} = .156 \left(\frac{x}{d} - 10 \right) \quad (2)$$

$$\left(\frac{U_0}{U_m} \right)^2 = .150 \frac{x}{d} \quad (3)$$

The quantity U_0 is the exit velocity. Note the difference in virtual origins for equations 2 and 3. This difference has been previously noted by Flora and Goldschmidt (1969) who indicated that the upstream turbulence is an important factor in determining the virtual origins and decay rate of the jet. No measurements were made of upstream turbulence. However, it is suggested, based on comparison with Flora and Goldschmidt's data, that in the present arrangement the turbulence level is low.

The Goertler solution for plane jets predicts that the mean cross flow velocity is given by equation (4).

$$\frac{\bar{\sigma V}}{U_m} = \frac{\sigma Y}{x} - \frac{\sigma Y}{x} \tanh^2 \frac{\sigma Y}{x} - .5 \tanh \frac{Y}{x} \quad (4)$$

where x is the distance from the kinematic virtual origin and in this case is equal to x . The term σ is obtained by solving equation 1 at the jet half width and is given by:

$$\sigma = \frac{x}{b} \arctan \frac{1}{\sqrt{2}} \quad (5)$$

Figure 2 shows plots of the Goertler solution and experimentally derived points. The scatter in these results is due in part to the difficulty of measuring low cross flow velocities at large $\frac{x}{d}$.

Measurements were made of the Reynolds stress components and the flatness (or 4th order term) of the fluctuating velocity components from $x/d = 20$ to $x/d = 60$. The measured shear stress was less than that calculated using similarity development of quantities involved. These results (not presented) showed good agreement with that published by previous authors (Heskestad 1965).

Variation of jet total pressure over the limited range had no effect on the normalized axial velocity curve. At low pressure ($Pr = 1.008$) the cross flow and Reynolds stress components were altered, particularly towards the edge of the jet. These measured quantities were small and could have been subjected to flow disturbances (e.g. wind) of the same magnitude as those naturally occurring in the jet.

4.3 Oscillating Vane

The principal results of introducing an oscillating vane are outlined below. The mean axial velocity profile is broadened and the centreline velocity value is decreased. The broadening increases with frequency and is in agreement with Collins, et al (1981). This is shown in Figure 3. These velocity profiles will normalize on the mean centreline velocity and jet half width for the frequencies and pressure ratios tested (Figure 4a). The normalized velocities have a profile that is rather more top hat in shape than the Goertler solution. The decay rate for the centreline velocity and the growth of the jet half width are both more rapid than for the corresponding steady jet and can be represented by equations (6) and (7) for the case of 40Hz oscillations.

$$\left(\frac{U_0}{U_m} \right)^2 = .48 \left(\frac{x}{d} - 5 \right) \quad (6)$$

$$\frac{b}{d} = .00462 \left(\frac{x}{d} \right)^2 + 325 \quad (7)$$

Note that the jet half width growth is parabolic, contrasting with the linear growth of the unexcited jet. The normalized cross flow velocity profile (Fig. 4b) is not significantly altered by the vane excitation.

Figure 5 shows representative plots of Reynolds stresses for the excited jet at $x/d = 40$. In contrast to the steady jet situation, turbulence values normalized on the centreline mean velocity do not collapse onto a single curve for various x/d locations. The u^2 turbulence intensity (Fig. 5a) is increased in the core region of the jet, the effect decreasing with downstream location. The v^2 turbulence intensity (Figure 5b) is increased throughout the jet, the effect increasing with downstream location. The peak Reynolds shear stress (Figure 5c) is increased in value throughout the measured regime. This effect has also been noticed in the wake of an oscillating airfoil, Degradé et al (1979).

Turbulence intensities, however, tend to disguise the real picture, since they have been obtained by normalizing on the centreline velocity - a quantity that is decaying at different rates in the steady and unsteady situations. Examination of the non-normalized u^2 turbulence levels (Figure 6) reveals that the v^2 turbulence level is increased considerably, (approx. 100% at $x/d = 40$) the effect decaying with increasing x/d . This represents a considerable increase in turbulent energy in the locations near the jet exit since not only is the turbulence level higher than that of the steady jet, but the region over which this turbulence exists has also increased due to the increase in jet width.

Flatness curves (not presented) for the fluctuating u and v components have similar shapes for both the excited and unexcited jet and, in the centre of the jet, values are typical of a gaussian rather than a sinusoidal process. The above effects are accompanied by an increase in jet entrainment (Figure 7) for the jet excited by the oscillating vane above that of the unexcited jet.

5. DISCUSSION

The exact mechanism that results in the above effects is not clear. It is postulated however that they result from coherent structures convected downstream through the turbulent field of the jet. Sato (1960) observed naturally occurring oscillations in the velocity field

of a plane jet. Cervantes and Goldschmidt (1980) observed a similar phenomenon, described as an apparent natural flapping motion of the jet, occurring at a local Strouhal number of 0.11 based on the local centre-line mean velocity and local half width of the jet, and attributed it to a local large scale motion resulting from an organized coherent structure within the jet's turbulent field. These observations appear consistent with the processes of vortex formation, growth and coalescence identified by Rockwell (1972); processes which can occur naturally at frequencies corresponding to the relevant Strouhal number, or which can be forced by transverse periodic disturbances in the initial formation region of the jet. This concept has been extended by Ho and Huang (1982) and Oster and Wagnanski (1982) who observed that the natural process of eddy formation and coalescence in a turbulent mixing layer can be substantially enhanced by sub-harmonic forcing techniques.

Conditionally sampled mean velocity profiles measured in the present experiments (Figure 8) also indicate an apparent flapping motion of the vane excited jet. Although the vane oscillation frequency was some two orders lower than the natural flapping frequency based on the above Strouhal number near the jet exit, the possibility of sub-harmonic forcing of vortex coalescence cannot be overlooked since both frequencies are of the same order further downstream where the present measurements were taken. To throw further light on this question and delineate the precise large scale motion generated by the oscillating vane, detailed flow visualization and more extensive conditionally sampled velocity measurements are required.

CONCLUSIONS

An oscillating vane located in the potential core of a two-dimensional jet is an effective method of increasing jet entrainment. The process appears to result from manipulation of the naturally occurring vortex structure of the jet. More detailed measurements and flow visualization are needed for a complete understanding of the vane-excited jet flow.

REFERENCES

- CERVANTES de GOTARI, J.G. and GOLDSCHMIDT, V.W. (1981) *J. Fluid Eng.* V103, pp 119 - 126.
- COLLINS, D.J., PLATZER, M.F., LAI, J.C.S. and SIMMONS, J.M. (1981) "Experimental Investigation of Oscillating Subsonic Jets", Proceedings of Symposium on Numerical and Physical Aspect of Aerodynamic Flows, California State University, Long Beach, CA, Jan. 1981.
- DeGRANDE, G., HAVERBEKE, A. and HIRSCH, Ch., (1979) "Digital Processing of Unsteady Periodic Signals with Application to the Turbulence Structure Around Oscillating Airfoils", ICIASF Congress on Instrumentation in Aerospace Simulation Facilities, Monterey, California, Published by IEEE, New York, 1979.
- DURST, F., MELLING, A. and WHITELOW, J.H. (1976) "Principles and Practice of Laser-Doppler Anemometry. Academic Press.
- GOLDSCHMIDT, W.V. and ESKINAZI, S. (1965) *J. Appl.Mech. ASME*, pp. 735-747.
- FIEDLER, H. and KORSCHULT, D. "The Two-Dimensional Jet with Periodic Initial Condition" 2nd Symposium on Turbulent Shear Flows, Imperial College, July 1979.
- FLORA, J.J. and GOLDSCHMIDT, V.W. (1969) *AIAA Journal*, Vol. 7, pp. 2344-2346.
- HESKERSTAD, G. (1965) *Trans ASME, J.Appl. Mech.* pp.1-14.
- HO C-M and HUANG L-S (1982) *J. Fluid Mech.* Vol. 119, pp. 443-473.

OSTER, D. and WYGNANSKI, I. (1982) *J. Fluid Mech.*123, 91.

ROCKWELL, D.O., (1972) *J. App.Mech.* 39, 833.

SATO, H. (1960) *J. Fluid Mech.* 7, 53.

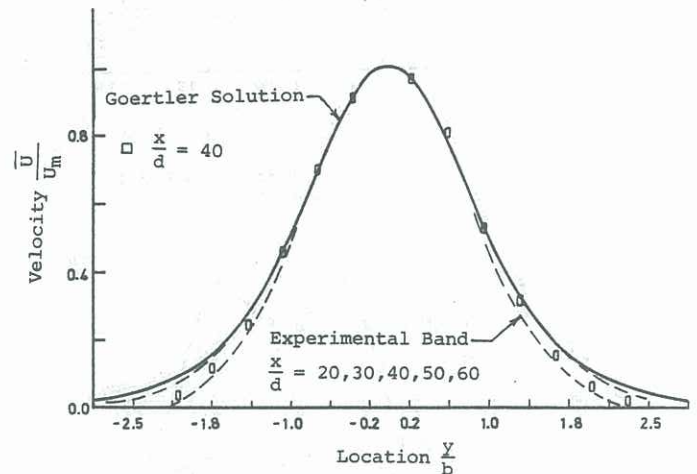


Figure 1 Steady Jet Mean Axial Velocity Profile

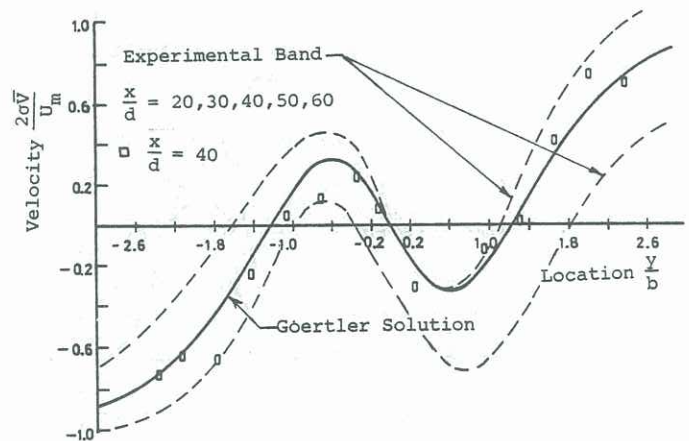


Figure 2 Steady Jet Mean Cross Flow Velocity Profile

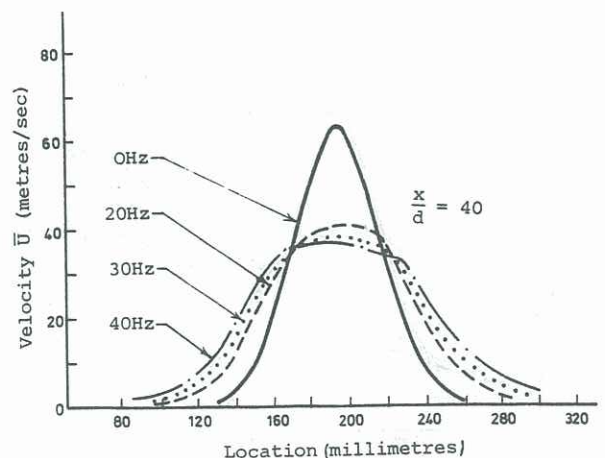


Figure 3 Effect of Vane Oscillations on Mean Axial Velocity

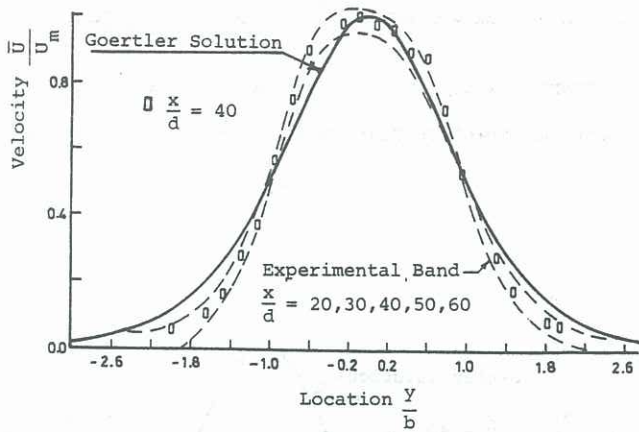


Figure 4a Excited Jet (40Hz) Mean Axial Velocity Profile

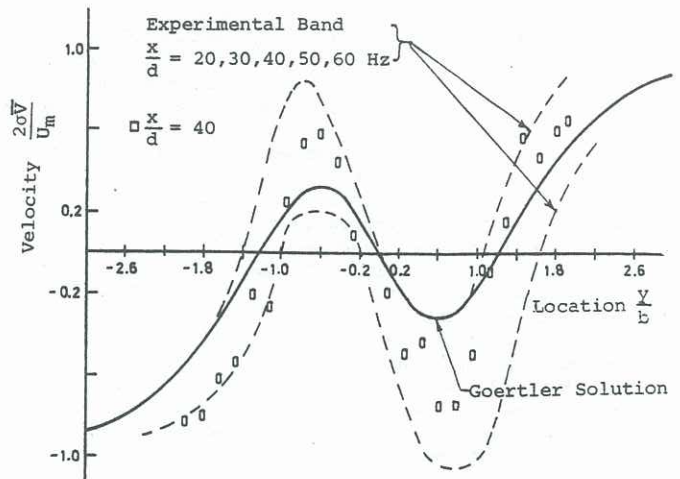


Figure 4b Excited Jet (40Hz) Mean Crossflow Velocity Profile

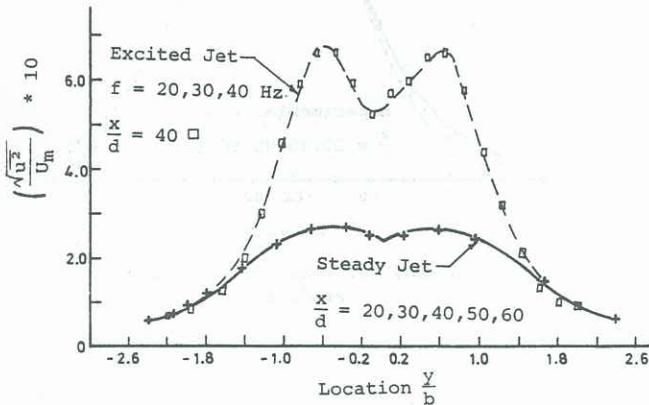


Figure 5a Lateral Distribution of Axial Turbulence

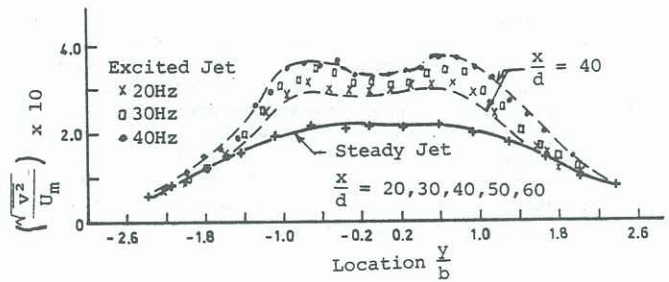


Figure 5b Lateral Distribution of Crossflow Turbulence

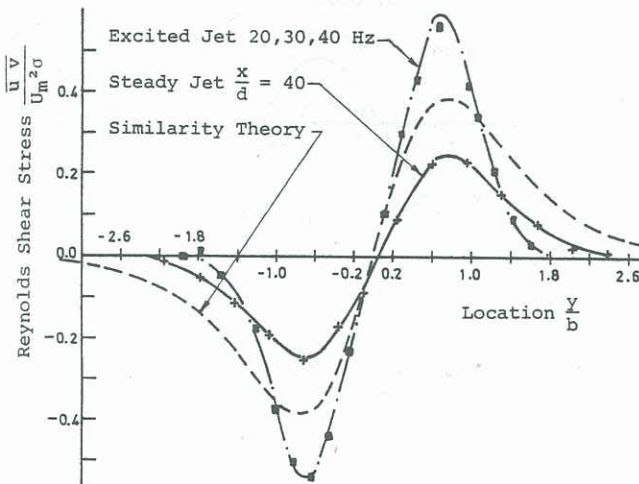


Figure 5c Lateral Distribution of Reynolds Shear Stress

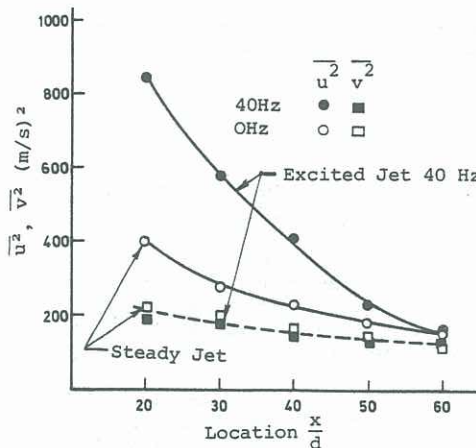


Figure 6 Centreline Turbulence Levels

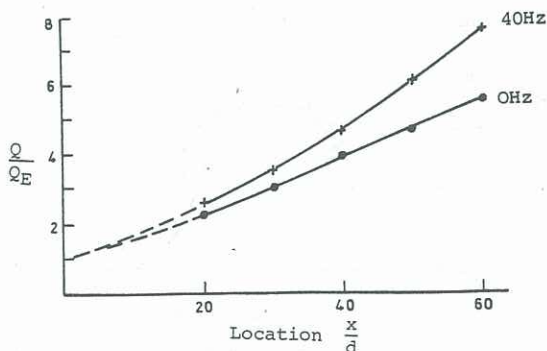


Figure 7 Entrainment Rate

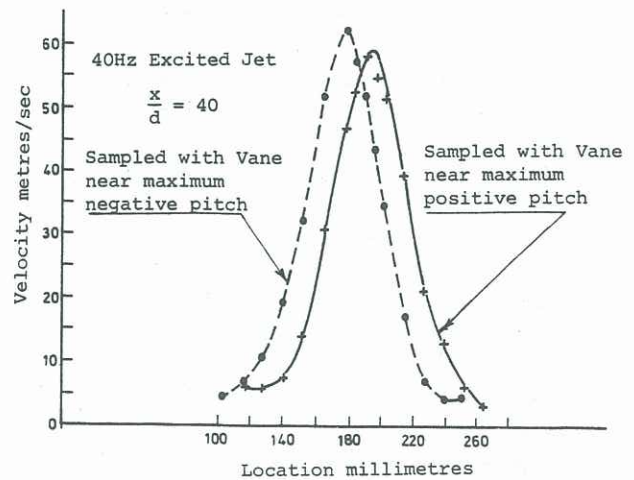


Figure 8 Apparent Flapping Motion of Excited Jet